

# Electric fatigue in antiferroelectric $\text{Pb}_{0.97}\text{La}_{0.02}(\text{Zr}_{0.55}\text{Sn}_{0.33}\text{Ti}_{0.12})\text{O}_3$ ceramics induced by bipolar cycling

Longjie Zhou\*, Georg Rixecker, André Zimmermann<sup>1</sup>, Fritz Aldinger

*Powder Metallurgy Laboratory, Max-Planck-Institut für Metallforschung and Institut für Nichtmetallische Anorganische Materialien, Universität Stuttgart, Pulvermetallurgisches Laboratorium, Heisenbergstrasse 3, D-70569 Stuttgart, Germany*

Received 24 August 2004; received in revised form 30 November 2004; accepted 5 December 2004

Available online 13 February 2005

## Abstract

Antiferroelectric lead zirconate titanate stannate (PZST) ceramics are promising materials for high-strain transducers and actuators. The degradation of the strain excited by an ac field remains largely unknown so far for this family of antiferroelectric ceramics. In this study, the bipolar electric fatigue of antiferroelectric  $\text{Pb}_{0.97}\text{La}_{0.02}(\text{Zr}_{0.55}\text{Sn}_{0.33}\text{Ti}_{0.12})\text{O}_3$  ceramics was investigated. Variations in the strain hysteresis loop and damage in the microstructure of the materials due to the electric cycling were monitored. Higher cycling field yielded a stronger fatigue effect. The material showed an increasingly asymmetric suppression of the strain hysteresis loop and diffuse AFE–FE phase transition with increasing cycle number. A damaged microstructure was observed on the polished surfaces of fatigued samples after acid etching. Electrochemical variations, the pinning of domains, randomly or preferentially orientated, due to the cycling are considered as the main fatigue mechanism of the material.

© 2005 Elsevier Ltd. All rights reserved.

**Keywords:** Microstructure; Fatigue;  $(\text{Pb},\text{La})(\text{Zr},\text{Sn},\text{Ti})\text{O}_3$

## 1. Introduction

The lead zirconate stannate titanate (PZST) family of ceramics, with  $\text{La}^{3+}$ ,  $\text{Nb}^{3+}$ ,  $\text{Sr}^{2+}$ ,  $\text{Ba}^{2+}$  and  $\text{Mg}^{2+}$  as dopants, has been studied for more than 30 years. The attractive feature of this class of materials originates from the fact that there is a large electrically induced longitudinal strain due to the phase transition from the tetragonal antiferroelectric to the rhombohedral ferroelectric phase provided that the antiferroelectric composition is located in the vicinity of the morphotropic phase boundary between the antiferroelectric and ferroelectric phases.<sup>1,2</sup> These materials, therefore, have been investigated for high strain transducers and actuators.<sup>3–5</sup> The materials could also be used as charge storage capacitors since the field forced ferroelectrics release all polariza-

tion charges and therefore can supply very high instantaneous current at the inversion of the phase transition, from the ferroelectric to the antiferroelectric state.<sup>6,7</sup> Like ferroelectric materials, the antiferroelectric PZST ceramics, show degradations in polarization and field induced strains when cycled under high ac fields. This fatigue effect has been mechanically and electrically the major hindrance for applications of the ceramics.<sup>8</sup>

Intensive investigations have been conducted to reveal the electric fatigue behaviour and mechanisms, mostly on ferroelectric bulk materials and thin films rather than on antiferroelectric ones, for more than a dozen years. Fatigue could be initiated by various factors, including intrinsic characteristics of the materials and extrinsic contributions. The former include the composition and microstructure of the bulk materials or thin films; the latter include surface condition, electrodes and temperature as well as the frequency, strength and type of the cycling field. Four stages of electric fatigue have been identified, including an incubation period, a stage of logarithmic fatigue, a saturation regime, and a recovery

\* Corresponding author. Tel.: +49 711 6893233; fax: +49 711 6893131.

E-mail address: [zhoulongjie@tsinghua.org.cn](mailto:zhoulongjie@tsinghua.org.cn) (L. Zhou).

<sup>1</sup> Present address: Robert Bosch GmbH, Corporate Research and Development.

stage.<sup>10,11</sup> There have been numerous models concerning the mechanisms of electric fatigue, including those related to electrochemical variations and mechanical deterioration.<sup>11</sup> The former are based on the scenario that domains become inactive due to point defects pinning the domain walls.<sup>12–14</sup> The latter rests on the idea that microcracks reduce the local effective field or yield conductive corrosion pathways in the material, thus decreasing the number of domains which can switch in the proximity of such cracks.<sup>15,16</sup> The electrochemical variations can be relieved by heat treatment at temperatures exceeding 300–500 °C,<sup>17</sup> while the mechanical deterioration in fatigued samples cannot be recovered below sintering temperatures.

Polarization, strain or acoustic emissions (AE) are suitable means by which to investigate the electric fatigue behaviour of ferroelectric and antiferroelectric materials. The three properties have been monitored simultaneously to investigate the fatigue behaviour of PZT bulk materials induced by bipolar cycling.<sup>11</sup> Altogether, most previous studies on electric fatigue have been concerned with polarization, a few with strain, while AE studies are rare.

Interesting results have been shown in previous studies on the deterioration of strain hysteresis loops induced by electric cycling. The asymmetric degradation of the strain hysteresis has been previously reported for ferroelectric bulk materials,<sup>11,18</sup> thin films<sup>19</sup> and crystals.<sup>20</sup> The asymmetry of the strain hysteresis was first attributed to some remaining influence of the first poling in pre-poled samples.<sup>21–23</sup> An alternative explanation for the asymmetry in strain hysteresis loops is the existence of an unidirectional frozen-in polarization, termed “offset polarization”.<sup>11</sup> The size of the regions of frozen polarization in thin films is on the scale of micrometers, the same order as the grains of the PZT-films,<sup>19</sup> while the size of those exposed on [1 1 1]<sub>C</sub> surfaces of PZN-PT crystals is on a millimeter scale. No significant asymmetric degradation of the strain hysteresis due to electric cycling was previously detected in PZST antiferroelectric bulk materials having different compositions.<sup>24,25</sup> The variations of the strain hysteresis loops of the antiferroelectric ceramics due to electric cycling, however, are different from composition to composition.

The present study investigates electric fatigue in a new composition in the PZST family of antiferroelectric ceramics. The electric fatigue behaviour of the material and the influence of the cycling field on fatigue will be discussed. The fatigue behaviour and fatigue mechanism of this composition will be compared with those of the antiferroelectric ceramics with different compositions studied previously.

## 2. Experimental procedure

### 2.1. Sample preparation

The composition of the antiferroelectric ceramics investigated in this paper is  $\text{Pb}_{0.97}\text{La}_{0.02}(\text{Zr}_{0.55}\text{Sn}_{0.33}\text{Ti}_{0.12})\text{O}_3$ .

Samples were prepared by solid-state reactions and conventional sintering, using commercially available reagent-grade raw oxides, i.e. PbO, BaO,  $\text{La}_2\text{O}_3$ ,  $\text{ZrO}_2$ ,  $\text{SnO}_2$  and  $\text{TiO}_2$ , as starting materials. Firstly, the starting oxides were mixed and attrition milled in isopropanol for 6 h with small zirconia balls as milling media in order to increase their reactivity and to get intimately mixed materials. After drying, the mixtures were calcined at 850 °C for 5 h and attrition milled again for 6 h. The resulting powders were dried at 60 °C for 24 h and cold isostatically pressed at 200 MPa into disks of 14 mm in diameter and 2 mm in thickness. The disks were sintered in an oxygen atmosphere which is necessary to achieve dense samples, using a heating and cooling rate of 3 °C/min and a holding time of 2 h at 1150 and 1250 °C, respectively. In order to minimise the lead loss during sintering, the samples were heated inside a closed alumina crucible with a constant PbO pressure provided by tablets of a powder mixture of  $\text{PbZrO}_3$ –8 wt.%  $\text{ZrO}_2$ . The average grain size and the relative density of the sintered samples are 2.6 μm and 98%, respectively. The samples were ground and fine polished to 1 μm finish into thin discs, about 0.5 mm in thickness, with flat and parallel major surfaces. Finally the samples were ground on the rim into round discs with 10 mm in diameter after annealing at 500 °C for 8 h in air and fully sputtering with gold as electrodes on both major surfaces.

### 2.2. Electric cycling and measurements

An inductive strain gauge was employed to measure the field induced longitudinal strain in the center of the disc samples immersed in silicone oil to prevent arcing. Sinusoidal fields with a frequency of 0.05 Hz were used for the measurements. The strain referred to in this paper is the longitudinal field induced strain.

The maximum values of the bipolar cycling fields were chosen as 3.5 and 4.5 kV/mm, which are about 1 and 2 kV/mm higher than the antiferroelectric to ferroelectric transition field (of 2.5 kV/mm), respectively. An electric transmitter provided the required sinusoidal voltage (50 Hz) from the normal electric line voltage for the electric cycling. Samples were immersed in a bath of silicone oil in order to avoid arcing and to ensure good thermal conductivity. The cycling field was slowly and steadily increased and decreased when loading and unloading. The starting and ending time of cycling were determined as the times when the field strength passed the value of 2.5 kV/mm. After a certain period of cycling, the samples were removed from the cycling set-up for strain hysteresis loop measurements under sinusoidal fields with the same maximum strength as in case of the corresponding cycling fields. Cycling and strain hysteresis loop measurements were repeated till a cycle number larger than  $10^8$  was reached. The strain hysteresis loop measurements were conducted again after a heat treatment of the fatigued samples at 500 °C for 1 h with heating and cooling rates of 5 °C/min.

The microstructure of the fatigued samples was observed by optical microscopy (Leica DM RM, Leica Microsystems

AG, Germany) on the polished surface about 100  $\mu\text{m}$  underneath the electrodes, and by scanning electron microscopy (SEM, JEOL 6300F) after etching of the surfaces. A solution of 5 ml of HCl and 95 ml of distilled water, containing a few drops of HF acid, was used as etchant. A few seconds of exposure gave clear images of the grains. The microstructures of virgin samples were observed in an identical way as references.

### 3. Results

The strain hysteresis loops of virgin samples, recorded with a maximum field of 3.5 and 4.5 kV/mm, are shown in Fig. 1(a) and (b), respectively. The loops are typical for antiferroelectric materials, showing a normal antiferroelectric–ferroelectric (AFE–FE) phase transition with a sudden increase in field induced strain at the transition field ( $E_{AF}$ ) of 2.5 kV/mm. The back switching from ferroelectric to antiferroelectric state (FE–AFE) exhibits a diffuse behaviour, with a transition field ( $E_{FA}$ ) in the range of 0.1–0.5 kV/mm. The diffuse nature of the FE–AFE phase transition is assumed to be related to microstresses in the field forced ferroelectric state due to the field induced strain since the FE–AFE transition can also be induced by pressure.

Fig. 1(c)–(f) show strain hysteresis loops of the materials cycled at 3.5 and 4.5 kV/mm for  $10^{6.5}$  and  $10^8$  cycles, respectively. Comparing Fig. 1(c) and (e) with Fig. 1(a) and Fig. 1(d) and (f) with Fig. 1(b), it is found that the strain hysteresis loop of the material exhibits remarkable variations in two aspects due to the bipolar electric cycling. On the one hand, the maximum strain is degraded asymmetrically with increasing cycle number. The asymmetry is caused by two different processes. Firstly, the whole loop is always shifted to the right into the direction of positive electric fields. Secondly, the maximum strain observed in the left wing ( $S_l$ ) of

the hysteresis loop is always higher than in the opposite direction (right wing  $S_r$ ). The direction of the asymmetry due to cycling is always the same. On the other hand, both the AFE–FE phase transition and its reverse transition become more diffuse with electric cycling. As shown in Fig. 1(a) and (b), the phase transitions of virgin samples exhibit normal behaviour with a clearly defined transition field and a sudden increase in strain at this field strength. After cycling of the samples for  $10^{6.5}$  times, the phase transition takes place in a field range rather than at a particular electric field, with its onset lower and its termination higher than 2.5 kV/mm. The reverse transition becomes more diffuse compared with that in the virgin state. The extent of the diffuseness of the phase transitions at the same cycle number varies from sample to sample, but shows an increasing trend with the cycle number for each sample. It cannot, however, be quantified so far.

Summarizing, the strain hysteresis loops exhibit not only an asymmetric degradation of the maximum strain, but also a diffuse nature of the AFE–FE phase transition and an enhancement in the diffuse character of the FE–AFE phase transition. Those variations increase with increasing cycle number.

Since the maximum strains of the left and right half measuring cycle,  $S_l$  and  $S_r$ , could always be identified exactly in strain hysteresis loops with cycle numbers from zero up to  $10^8$ , these two parameters and the gap between them,  $\Delta S$ , are used to characterize the fatigue behaviour of the material.  $S_l$ ,  $S_r$  and  $\Delta S$  as a function of cycle number under both magnitudes of the cycling fields are shown in Fig. 2, while the normalized  $S_l$ ,  $S_r$  and  $\Delta S$  are presented in Fig. 3. For the normalization, the respective maximum strain in the virgin state is utilized. The maximum strains exhibit degeneration starting at around  $10^5$  cycles, undergo logarithmic fatigue after  $10^5$  cycles and show no indication of recovery till  $10^8$  cycles. The degradation of  $S_r$  with increasing cycle number is always more pronounced than that of  $S_l$ . In the

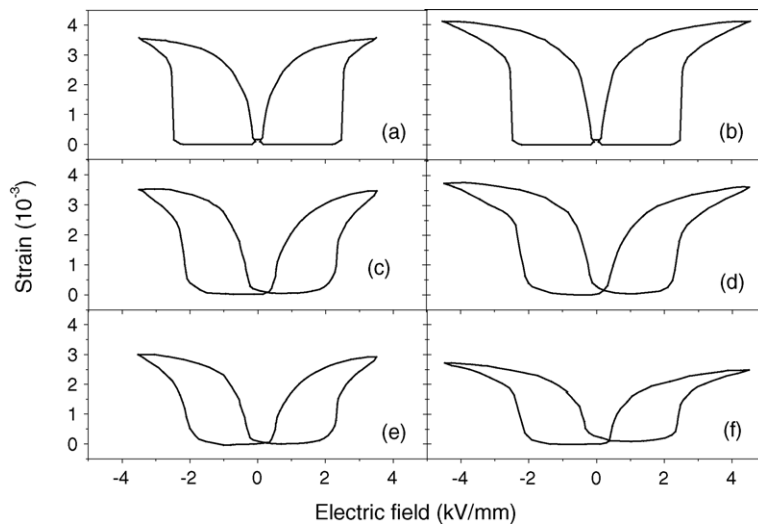


Fig. 1. Strain hysteresis loops of a measuring cycle for the samples: in virgin state with a maximum field of 3.5 kV/mm (a) or 4.5 kV/mm (b); cycled for  $10^{6.5}$  times at 3.5 kV/mm (c) or 4.5 kV/mm (d); and cycled for  $10^8$  times at 3.5 kV/mm (e) or at 4.5 kV/mm (f).

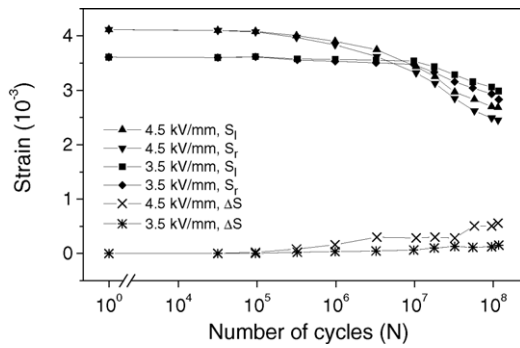


Fig. 2.  $S_1$ ,  $S_r$  and  $\Delta S$  as a function of cycle number.

virgin state, the strain hysteresis loops are symmetric, with maximum strains,  $3.61 \times 10^{-3}$  and  $4.12 \times 10^{-3}$  at 3.5 and 4.5 kV/mm, respectively. After cycling at 3.5 and 4.5 kV/mm for  $10^{5.5}$  cycles, the maximum strains show a significant decrease with obvious asymmetry in both cases.  $S_1$  and  $S_r$  decrease more strongly at high cycling field than at low cycling field. The degeneration accelerates with rising cycle number. When the cycle number reaches  $10^8$ ,  $S_1$  and  $S_r$  are reduced by  $1.42 \times 10^{-3}$  (34.5%) and  $1.63 \times 10^{-3}$  (39.6%) with the cycling field of 4.5 kV/mm, while the reduction amounts to  $5.5 \times 10^{-4}$  (15.2%) and  $6.8 \times 10^{-4}$  (18.8%) at 3.5 kV/mm.  $\Delta S$  at both cycling fields shows a rising trend with the cycle number, indicating an increasing asymmetry of the strain hysteresis loop. In general, a higher cycling field yields a larger  $\Delta S$ .

By the use of optical microscopy, no significant damage was observed in the microstructure on the polished surfaces

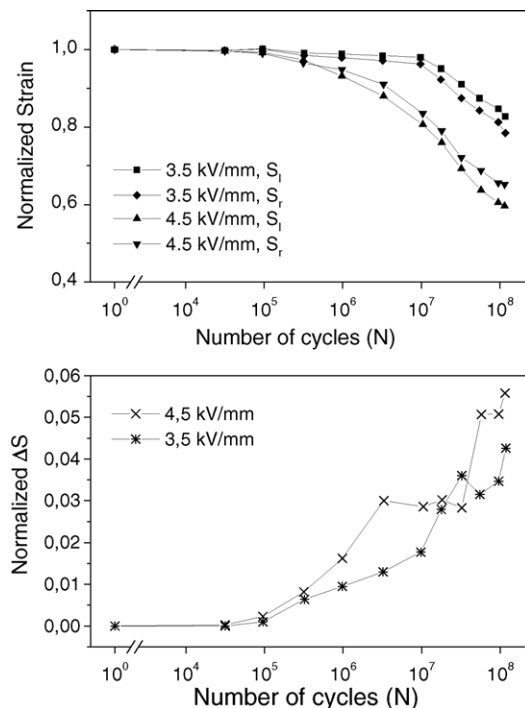


Fig. 3. Normalized  $S_1$ ,  $S_r$  and  $\Delta S$  values as a function of cycle number.

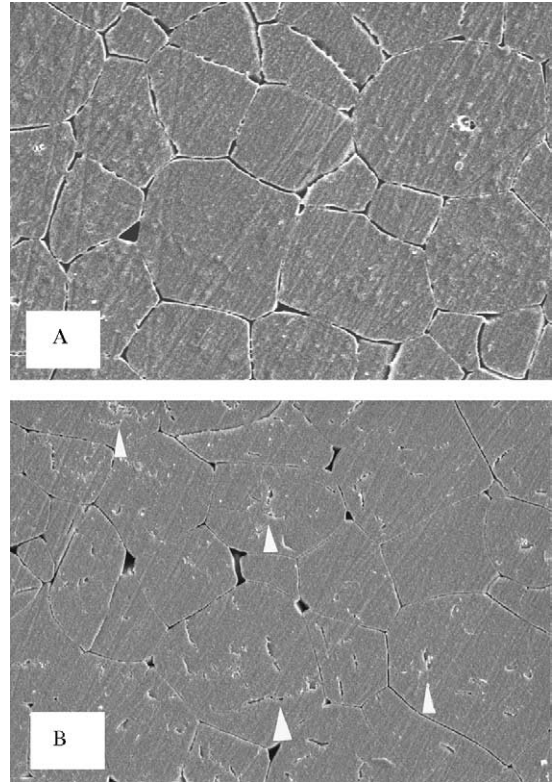


Fig. 4. Micrograph of the polished-etched surface for (A) the virgin sample and (B) the samples cycled at 4.5 kV/mm for  $10^8$  cycles (some etch grooves are marked).

of the fatigued samples. There were no macro and microcracks noticeable on the surfaces. Significant microstructural modifications, however, were found via SEM observation of the polished-etched surfaces of the fatigued material. Numerous etch grooves can be found within grains, as shown in Fig. 4(B). In contrast, there is no such etch grooves noticeable within grains of the virgin microstructure (Fig. 4(A)).

Fig. 5 shows the strain hysteresis loop for the fatigued-recovered state (bold curve) of a sample cycled at 4.5 kV/mm for  $10^8$  cycles and recovered by heat treatment at  $500^\circ\text{C}$  for 1 h. The strain hysteresis loop for the virgin state (fine

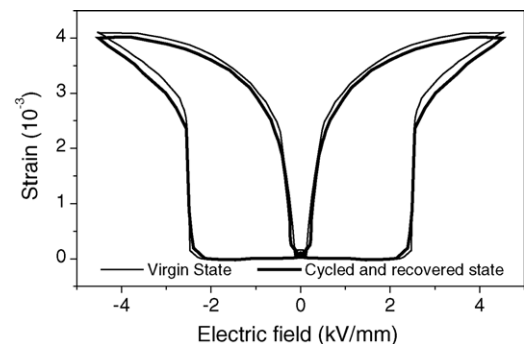


Fig. 5. The strain hysteresis loop (bold curve) for a fatigued-recovered sample (cycled at 4.5 kV/mm for  $10^8$  cycles and resumed by heat treatment at  $500^\circ\text{C}$  for 1 h).

curve) of the sample, shown in Fig. 1(b), is also plotted in Fig. 5 for comparison. Compared with the virgin loop, the strain hysteresis loop for the fatigued-recovered state shows a remarkable degree of recovery. The symmetry of the strain hysteresis loop was re-established. The AFE–FE transition field resumed its initial value, while the diffuse character of AFE–FE phase transition due to cycling disappeared. The FE–AFE phase transition was also almost recovered to its original behaviour. The AFE–FE transition strain and the maximum strain, however, were not fully restored to their original values. Nevertheless, it is evident from the hysteresis loop that the recovery of the fatigued sample was almost complete.

#### 4. Discussion

When the cycle number exceeds  $10^8$ , the fatigue of PZT ferroelectric bulk materials, as evidenced by the field-induced strain, shows four stages.<sup>11</sup> This agrees with the stages of fatigue of polarization in ferroelectric bulk materials as well as thin films.<sup>9–11</sup> The stages of electric fatigue for antiferroelectric ceramics have not yet been fully understood, but it is assumed that these materials will undergo similar fatigue stages to the ferroelectric ones. According to the degradation of the maximum strain with the cycle number, the antiferroelectric fatigue in this study undergoes the stages from the incubation to the logarithmic period or, at most, to a saturation state under both cycling fields since there is no indication of recovery of the maximum strains even when at  $10^8$  cycles.

The fatigue was found to strongly depend on the strength of the cycling field. Higher cycling field yields stronger fatigue effect, and, thus, more degeneration in the maximum field induced strain and more diffusion of the AFE–FE phase transition. This is consistent with previously published results on both ferroelectric and antiferroelectric materials.<sup>11,24,26,27</sup> According to electrochemical mechanisms, electric fatigue results from the pinning of domain walls by charged species that migrate or reorient from their initially random positions or direction to the preferred sites or orientations driven by an applied electric field. A higher cycling field provides a stronger driving force to yield a more severe fatigue effect.

So far, numerous mechanisms for electric fatigue have been proposed, as summarized by Nuffer et al.<sup>11</sup> Those models are concerned with both mechanical deterioration and electrochemical variations. It is clear in this study that the antiferroelectric to ferroelectric phase transition and the reverse transition are also a driving mechanism for the electric fatigue since the transitions are accompanied by large changes in strain and consequent microstress, which is expected to cause mechanical deterioration during cycling. The effect of the phase transitions on mechanical deterioration in this material is not as pronounced as in a material with a different composition of  $(\text{Pb}_{0.97}\text{La}_{0.02}(\text{Zr}_{0.77}\text{Sn}_{0.14}\text{Ti}_{0.09})\text{O}_3)$ , which was examined earlier. Cycled for  $10^8$  times under the same maximum value of electric field, the latter material exhibited

a severely deteriorated microstructure detectable by optical microscopy,<sup>25</sup> while the present one shows significant damages in the microstructure due to the cycling only after acid etching of the polished surface. The diffuse AFE–FE phase transition in the present material rather than a normal one in the earlier investigation shows a gradual transition strain without a sudden change and, thus, has less impact on the microstructure. Electrochemical variation rather than mechanical deterioration is considered to be the main fatigue mechanism for the present material since the symmetry of the strain hysteresis loop and the normal AFE–FE phase transition are recovered after heat treatment of the fatigued samples.

It is assumed that the pinning of domains contributes to the diffuse AFE–FE phase transition of the material caused by electric cycling. After a period of cycling, some domains are pinned by charged species, and a higher energy, i.e. a higher electric field is needed to cause the AFE–FE phase transition. The energy needed for the phase transition of individual domains is distributed over a range of electric fields and, thus, results in the diffuse phase transition. It is possible that some domains are frozen so strongly that a small fraction of field forced ferroelectric phase is not relieved into the antiferroelectric state when the electric field decreased to zero. Those ferroelectric domains, however, are reoriented when driven by electric field, which is also likely to contribute to the diffuse character of the AFE–FE transition.

There are alternative scenarios for the asymmetric degradation of the strain hysteresis due to electric cycling. One is related to a preferred poling direction in ferroelectric materials,<sup>21–23</sup> the second is attributed to the existence of a unidirectional frozen polarization, termed “offset polarization”.<sup>11,28–30</sup> Since there is no preferential orientation of domains in the virgin antiferroelectric ceramics before cycling, the former hypothesis is excluded as the source of strain hysteresis asymmetry. The hypothesis of offset polarization is consistent with the observation of special regions with a strong preferential direction of the frozen polarization domains by atomic force microscopy (AFM).<sup>19</sup> Kholkin et al.<sup>28</sup> reported a direct measurement of offset polarization for PZT thin films after bipolar cycling. Lupascu et al.<sup>11,30</sup> calculated the values of offset polarization due to electric cycling in a commercial PZT ferroelectric material (PIC 151, PI Ceramic, Lederhose, Germany) according to the Landau-Devonshire theory, assuming that the strain of the material is proportional to the square of the total polarization. These investigations support the scenario of pinning of ferroelectric domains in a preferred direction.

Two preferred directions of frozen polarization were indicated in polycrystalline compounds since the left wings of strain or piezoelectric hysteresis loops show more severe changes than the right one in fatigued PZT ferroelectric materials,<sup>11,28–30</sup> while the opposite type of strain hysteresis asymmetry was evidenced in another specific ferroelectric material<sup>23</sup> and the antiferroelectric material in this study. Both asymmetry types, however, can be found in fatigued PZN-PT crystals in the  $[1\ 1\ 1]_c$  orientation.

Different length scales of the areas with frozen polarization may contribute to the fact that only one type of asymmetry shows up in a given polycrystalline material, while different types are exhibited by single crystals. Two main configurations of frozen polarization domains were distinguished in PZT thin films.<sup>19</sup> One is characterized by a strong preferential direction and the other are by randomly distributed regions of oppositely oriented frozen polarization. The size of the regions in the PZT thin films is in the micrometer-range, the same order of magnitude as the size of the grains. The length scales of such regions in other polycrystalline materials are assumed to be similar to the grain sizes of the material, on the order of several micrometers. Such small regions make it impossible to monitor hysteresis loops region by region since the size of contact points on the electrodes of the materials for strain measurement is in a scale of, at least, hundreds of micrometers. In this case, the hysteresis loops detected show a combined effect of hundreds of frozen polarization regions, among which those in the preferential direction contribute to the asymmetry of the loop. The size of regions with different types of strain hysteresis asymmetry in single crystals was reported to be in the order of millimeters,<sup>20</sup> which may be the same scale as the frozen polarization regions. Such a large size makes it possible to monitor strain hysteresis loops region by region. Thus, opposite asymmetry types of strain hysteresis loops were recorded in oppositely-oriented frozen polarization regions.

## 5. Conclusions

Higher cycling field yields a stronger fatigue effect in the antiferroelectric PZST material. The ceramic shows asymmetric degeneration of field induced strain, a diffuse AFE–FE phase transition and mechanical damage in the microstructure due to the bipolar electric cycling. The changes in the strain hysteresis loop are attributed to electrochemical variations, such as the pinning of domains due to the cycling. More specifically, the pinning of some domains in a preferential direction results in an asymmetry of the strain hysteresis loop. Those variations are thermally unstable and can be recovered by heat treatments.

## Acknowledgements

The authors gratefully acknowledge financial support by the Deutsche Forschungsgemeinschaft. Mr. R. Mager's help in technical support is cordially appreciated.

## References

- Pan, W. Y., Dam, C. O., Zhang, Q. M. and Cross, L. E., Large displacement transducers based on electric field forced phase transitions in the tetragonal  $(\text{Pb}_{0.97}\text{La}_{0.02})(\text{Ti,Zr,Sn})$  family of ceramics. *J. Appl. Phys.*, 1989, **66**, 6014–6023.

- Shebanov, L., Kusnetsov, M. and Sternberg, A., Electric field-induced antiferroelectric-to-ferroelectric phase transition in lead zirconate titanate stannate ceramics modified with lanthanum. *J. Appl. Phys.*, 1994, **76**, 4301–4304.
- Pan, W., Zhang, Q., Bhalla, A. and Cross, L. E., Field-forced antiferroelectric-to-ferroelectric switching in modified lead zirconate titanate stannate ceramics. *J. Am. Ceram. Soc.*, 1989, **72**, 571–578.
- Bharadwaja, S. and Krupanidhi, S. B., Antiferroelectric thin films for MEMS applications. *Ferroelectricity*, 2001, **263**, 39–44.
- Wu, B., Ye, Y., Wang, Q. and Cross, L. E., Dependence of electrical properties on film thickness in lanthanum-doped lead zirconate titanate stannate antiferroelectric thin films. *J. Appl. Phys.*, 1999, **85**, 3753–3758.
- Aerlincourt, D., Krueger, H. H. A. and Jaffe, B., Stability of phases in modified lead zirconate with variation in pressure, electric field, temperature and composition. *J. Phys. Chem. Solids*, 1964, **25**, 659–674.
- Jaffe, B., Antiferroelectric ceramics with field-enforced transitions: a new nonlinear circuit element. *Proc. IRE*, 1961, **49**, 1264–1267.
- Jiang, Q. Y. and Cross, L. E., Effects of porosity on electric fatigue behaviour in PLZT and PZT ferroelectric ceramics. *J. Mater. Sci.*, 1993, **28**, 4536–4543.
- Pawlaczyk, C. Z., Tagantsev, A. K., Brooks, K., Reaney, I. M., Klisurska, R. and Setter, N., Fatigue, rejuvenation and self-restoring in ferroelectric thin films. *Integr. Ferroelectr.*, 1995, **8**, 283–316.
- Colla, E. L., Tagantsev, A. K., Taylor, D. V. and Kholin, A. L., Fatigued state of the Pt–PZT–Pt system. *Integr. Ferroelectr.*, 1997, **18**, 19–28.
- Nuffer, J., Lupascu, D. C. and Rödel, J., Damage evolution in ferroelectric PZT induced by bipolar electric cycling. *Acta Mater.*, 2000, **48**, 3783–3794.
- Robels, U., Schneider-Störmann, L. and Arlt, G., Dielectric aging and its temperature dependence in ferroelectric ceramics. *Ferroelectricity*, 1995, **168**, 301–311.
- Brennan, C., Model of ferroelectric fatigue due to defect/domain interactions. *Ferroelectricity*, 1993, **150**, 199–208.
- Tagantsev, A. K. and Stolichnov, I. A., Injection-controlled size effect on switching of ferroelectric thin films. *Appl. Phys. Lett.*, 1999, **74**, 1326–1328.
- Jiang, Q., Cao, W. and Cross, L. E., Electric fatigue in lead zirconate titanate ceramics. *J. Am. Ceram. Soc.*, 1994, **77**, 211–215.
- Duiker, H. M., Beale, P. D., Scott, J. F., Paz de Araujo, C. A., Milnick, B. M., Cuchiari, J. D. and Mcmillan, L. D., Fatigue and switching in ferroelectric memories: theory and experiment. *J. Appl. Phys.*, 1990, **68**, 5783–5791.
- Nuffer, J., Lupascu, D. C. and Rödel, J., Stability of pinning centers in fatigued lead-zirconate-titanate. *Appl. Phys. Lett.*, 2002, **80**, 1049–1051.
- Winzer, S. R., Shankar, N. and Ritter, A. P., Designing cofired multilayer electrostrictive actuators for reliability. *J. Am. Ceram. Soc.*, 1989, **72**, 2246–2257.
- Colla, E. L., Seungbum, H., Taylor, D. V., Tagantsev, A. K., Setter, N. and Kwangsoo, N., Direct observation of region by region suppression of the switchable polarization (fatigue) in  $\text{Pb}(\text{Zr,Ti})\text{O}_3$  thin film capacitors with Pt electrodes. *Appl. Phys. Lett.*, 1998, **72**, 2763–2765.
- Ozgul, M., Troler-McKinstry, S. and Randall, C. A., Influence of electrical cycling on polarization reversal processes in  $\text{Pb}(\text{Zn}_{1/3}\text{Nb}_{2/3})\text{O}_3$ – $\text{PbTiO}_3$  ferroelectric single crystals as a function of orientation. *J. Appl. Phys.*, 2004, **95**, 4296–4302.
- Warren, W. L., Tuttle, B. A. and Dimos, D., Ferroelectric fatigue in perovskite oxides. *Appl. Phys. Lett.*, 1995, **67**, 1426–1428.
- Warren, W. L., Dimos, D., Tuttle, B. A., Pike, G. E. and Al-Shareef, H. N., Relationships among ferroelectric fatigue, electronic charge trapping, defect-dipoles, and oxygen vacancies in perovskite oxides. *Integr. Ferroelectr.*, 1997, **16**, 77–86.
- Weitzing, H., Schneider, G. A., Steffens, J., Hammer, M. and Hoffmann, M. J., Cyclic fatigue due to electric loading in ferroelectric ceramics. *J. Eur. Ceram. Soc.*, 1999, **19**, 1333–1337.

24. Zhou, L., Zimmermann, A., Zeng, Y. and Aldinger, F., Bipolar electric fatigue behaviour as a function of field strength in antiferroelectric (Pb,Ba,La)(Zr,Sn,Ti)O<sub>3</sub> ceramics. *J. Mater. Sci.*, 2004, **39**, 2675–2681.
25. Zhou, L., Zimmermann, A., Zeng, Y. and Aldinger, F., Fatigue of field-induced strain in antiferroelectric Pb<sub>0.97</sub>La<sub>0.02</sub>(Zr<sub>0.77</sub>Sn<sub>0.14</sub>Ti<sub>0.09</sub>)O<sub>3</sub> ceramics. *J. Am. Ceram. Soc.*, 2004, **87**, 1591–1593.
26. Zhai, J. and Chen, H., Electric fatigue in Pb(Nb,Zr,Sn,Ti)O<sub>3</sub> thin films grown by a sol–gel process. *Appl. Phys. Lett.*, 2003, **83**, 978–980.
27. Mihara, T., Watanabe, H. and Paz de Araujo, C. A., Characteristic change due to polarization fatigue of sol–gel ferroelectric Pb(Zr<sub>0.4</sub>Ti<sub>0.6</sub>)O<sub>3</sub> thin-film capacitors. *Jpn. J. Appl. Phys.*, 1994, **33**(Part 1), 5281–5286.
28. Kholkin, A. L., Colla, E. L., Tagantsev, A. K., Taylor, D. V. and Setter, N., Fatigue of piezoelectric properties in Pb(Zr,Ti)O<sub>3</sub>. *Appl. Phys. Lett.*, 1996, **68**, 2577–2579.
29. Lupascu, D. C., Aulbach, E. and Rödel, J., Mixed electromechanical fatigue in lead zirconate titanate. *J. Appl. Phys.*, 2003, **93**, 5551–5556.
30. Verdier, C., Lupascu, D. C. and Rödel, J., Unipolar fatigue of ferroelectric lead-zirconate-titanate. *J. Eur. Ceram. Soc.*, 2003, **23**, 1409–1415.